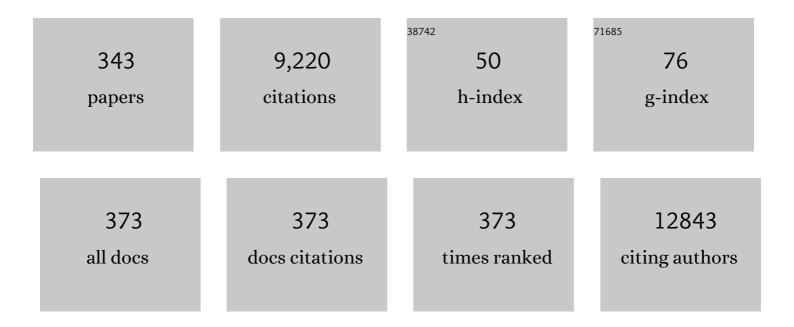
Manuel Desco

List of Publications by Year in descending order

Source: https://exaly.com/author-pdf/7654815/publications.pdf Version: 2024-02-01



#	Article	IF	CITATIONS
1	Goat Milk Exosomes As Natural Nanoparticles for Detecting Inflammatory Processes By Optical Imaging. Small, 2022, 18, e2105421.	10.0	25
2	Feto-maternal microchimerism: Memories from pregnancy. IScience, 2022, 25, 103664.	4.1	11
3	An Update on the Exploratory Use of Curcumin in Neuropsychiatric Disorders. Antioxidants, 2022, 11, 353.	5.1	14
4	A Novel Bayesian Linear Regression Model for the Analysis of Neuroimaging Data. Applied Sciences (Switzerland), 2022, 12, 2571.	2.5	2
5	Simple beam-hardening correction method (2DCalBH) based on 2D linearization. Physics in Medicine and Biology, 2022, , .	3.0	0
6	Neuroimaging reveals distinct brain glucose metabolism patterns associated with morphine consumption in Lewis and Fischer 344 rat strains. Scientific Reports, 2022, 12, 4643.	3.3	4
7	In vivo Positron Emission Tomography to Reveal Activity Patterns Induced by Deep Brain Stimulation in Rats. Journal of Visualized Experiments, 2022, , .	0.3	0
8	Local Functional Connectivity as a Parsimonious Explanation of the Main Frameworks for ADHD in Medication-NaÃ ⁻ ve Adults. Journal of Attention Disorders, 2022, 26, 1788-1801.	2.6	1
9	A 3D Analysis of Cleared Human Melanoma. Biomedicines, 2022, 10, 1580.	3.2	3
10	Optimization of a calibration phantom for quantitative radiography. Medical Physics, 2021, 48, 1039-1053.	3.0	4
11	Do Pregnancy-Induced Brain Changes Reverse? The Brain of a Mother Six Years after Parturition. Brain Sciences, 2021, 11, 168.	2.3	36
12	Super-Iterative Image Reconstruction in PET. IEEE Transactions on Computational Imaging, 2021, 7, 248-257.	4.4	4
13	Exploratory study ofÂthe long-term footprint of deep brain stimulation on brain metabolism and neuroplasticity in an animal model of obesity. Scientific Reports, 2021, 11, 5580.	3.3	5
14	Omega-3 fatty acids during adolescence prevent schizophrenia-related behavioural deficits: Neurophysiological evidences from the prenatal viral infection with PolyI:C. European Neuropsychopharmacology, 2021, 46, 14-27.	0.7	13
15	Effect of illumination level [18F]FDG-PET brain uptake in free moving mice. PLoS ONE, 2021, 16, e0251454.	2.5	0
16	A Characterization of the Effects of Minocycline Treatment During Adolescence on Structural, Metabolic, and Oxidative Stress Parameters in a Maternal Immune Stimulation Model of Neurodevelopmental Brain Disorders. International Journal of Neuropsychopharmacology, 2021, 24, 734-748.	2.1	11
17	Brillouin Spectroscopy: From Biomedical Research to New Generation Pathology Diagnosis. International Journal of Molecular Sciences, 2021, 22, 8055.	4.1	8
18	Corticospinal tract and motor cortex degeneration in pure hereditary spastic paraparesis type 4 (SPG4). Amyotrophic Lateral Sclerosis and Frontotemporal Degeneration, 2021, , 1-10.	1.7	5

#	Article	IF	CITATIONS
19	Tolerance to geometrical inaccuracies in CBCT systems: A comprehensive study. Medical Physics, 2021, 48, 6007-6019.	3.0	2
20	Covalently Labeled Fluorescent Exosomes for In Vitro and In Vivo Applications. Biomedicines, 2021, 9, 81.	3.2	15
21	Characterizing the Brain Structural Adaptations Across the Motherhood Transition. Frontiers in Global Women S Health, 2021, 2, 742775.	2.3	18
22	Positron Emission Tomography of the. Neuromethods, 2021, , 281-305.	0.3	0
23	Assessment of myocardial viscoelasticity with Brillouin spectroscopy in myocardial infarction and aortic stenosis models. Scientific Reports, 2021, 11, 21369.	3.3	3
24	Simplified Statistical Image Reconstruction for X-ray CT With Beam-Hardening Artifact Compensation. IEEE Transactions on Medical Imaging, 2020, 39, 111-118.	8.9	9
25	Sensory-to-Cognitive Systems Integration Is Associated With Clinical Severity in Autism Spectrum Disorder. Journal of the American Academy of Child and Adolescent Psychiatry, 2020, 59, 422-433.	0.5	33
26	Evaluation of Clostridium difficile Infection with PET/CT Imaging in a Mouse Model. Molecular Imaging and Biology, 2020, 22, 587-592.	2.6	5
27	Intraoperative computed tomography imaging for dose calculation in intraoperative electron radiation therapy: Initial clinical observations. PLoS ONE, 2020, 15, e0227155.	2.5	6
28	Becoming a mother entails anatomical changes in the ventral striatum of the human brain that facilitate its responsiveness to offspring cues. Psychoneuroendocrinology, 2020, 112, 104507.	2.7	50
29	Biomedical Applications of Tissue Clearing and Three-Dimensional Imaging in Health and Disease. IScience, 2020, 23, 101432.	4.1	67
30	Structural and Functional Brain Abnormalities in Mouse Models of Lafora Disease. International Journal of Molecular Sciences, 2020, 21, 7771.	4.1	4
31	The Paternal Transition Entails Neuroanatomic Adaptations that are Associated with the Father's Brain Response to his Infant Cues. Cerebral Cortex Communications, 2020, 1, tgaa082.	1.6	9
32	Single breath-hold saturation recovery 3D cardiac T1 mapping via compressed SENSE at 3T. Magnetic Resonance Materials in Physics, Biology, and Medicine, 2020, 33, 865-876.	2.0	5
33	T cells with dysfunctional mitochondria induce multimorbidity and premature senescence. Science, 2020, 368, 1371-1376.	12.6	286
34	Radioactive Labeling of Milk-Derived Exosomes with 99mTc and In Vivo Tracking by SPECT Imaging. Nanomaterials, 2020, 10, 1062.	4.1	41
35	Accelerated iterative image reconstruction for cone-beam computed tomography through Big Data frameworks. Future Generation Computer Systems, 2020, 106, 534-544.	7.5	3
36	Real-Time 3D PET Image with Pseudoinverse Reconstruction. Applied Sciences (Switzerland), 2020, 10, 2829.	2.5	6

#	Article	IF	CITATIONS
37	Association of visual and quantitative heterogeneity of 18F-FDG PET images with treatment response in locally advanced rectal cancer: A feasibility study. PLoS ONE, 2020, 15, e0242597.	2.5	9
38	Effects of a Ketogenic Diet on [18F]FDG-PET Imaging in a Mouse Model of Lung Cancer. Molecular Imaging and Biology, 2019, 21, 279-285.	2.6	6
39	Stepwise functional connectivity reveals altered sensoryâ€multimodal integration in medicationâ€naÃ⁻ve adults with attention deficit hyperactivity disorder. Human Brain Mapping, 2019, 40, 4645-4656.	3.6	14
40	Magnetic Nanoplatelets for High Contrast Cardiovascular Imaging by Magnetically Modulated Optical Coherence Tomography. ChemPhotoChem, 2019, 3, 503-503.	3.0	0
41	FP456COGNITIVE FUNCTION, HIPPOCAMPUS AND HYPERPARATHYROIDISM IN ADVANCED CKD. Nephrology Dialysis Transplantation, 2019, 34, .	0.7	0
42	Pregnancy and adolescence entail similar neuroanatomical adaptations: A comparative analysis of cerebral morphometric changes. Human Brain Mapping, 2019, 40, 2143-2152.	3.6	60
43	Applications of Light-Sheet Microscopy in Microdevices. Frontiers in Neuroanatomy, 2019, 13, 1.	1.7	81
44	Risperidone administered during adolescence induced metabolic, anatomical and inflammatory/oxidative changes in adult brain: A PET and MRI study in the maternal immune stimulation animal model. European Neuropsychopharmacology, 2019, 29, 880-896.	0.7	27
45	XAP-Lab: A software tool for designing flexible X-ray acquisition protocols. Computer Methods and Programs in Biomedicine, 2019, 177, 243-252.	4.7	1
46	Magnetic Nanoplatelets for High Contrast Cardiovascular Imaging by Magnetically Modulated Optical Coherence Tomography. ChemPhotoChem, 2019, 3, 529-539.	3.0	16
47	Vascular smooth muscle cellâ€specific progerin expression in a mouse model of Hutchinson–Gilford progeria syndrome promotes arterial stiffness: Therapeutic effect of dietary nitrite. Aging Cell, 2019, 18, e12936.	6.7	51
48	CIBERSAM: Ten years of collaborative translational research in mental disorders. Revista De PsiquiatrÃa Y Salud Mental (English Edition), 2019, 12, 1-8.	0.3	5
49	Assessment of the anti-biofilm effect of micafungin in an animal model of catheter-related candidemia. Medical Mycology, 2019, 57, 496-503.	0.7	3
50	Chemoenzymatic radiosynthesis of 2-deoxy-2-[18F]fluoro-d-trehalose ([18F]-2-FDTre): A PET radioprobe for in vivo tracing of trehalose metabolism. Carbohydrate Research, 2019, 472, 16-22.	2.3	29
51	Diez años de investigación traslacional colaborativa en enfermedades mentales: el CIBERSAM. Revista De PsiquiatrÃa Y Salud Mental, 2019, 12, 1-8.	1.8	68
52	Impact of optical tissue clearing on the Brillouin signal from biological tissue samples. Biomedical Optics Express, 2019, 10, 2674.	2.9	5
53	The Paracrine Neural Stem Cell Niche: New Actors in the Play. Current Stem Cell Reports, 2018, 4, 33-38.	1.6	3
54	Local functional connectivity suggests functional immaturity in children with attentionâ€deficit/hyperactivity disorder. Human Brain Mapping, 2018, 39, 2442-2454.	3.6	35

#	Article	IF	CITATIONS
55	Improving PET Quantification of Small Animal [68Ga]DOTA-Labeled PET/CT Studies by Using a CT-Based Positron Range Correction. Molecular Imaging and Biology, 2018, 20, 584-593.	2.6	20
56	Functionalization and Characterization of Magnetic Nanoparticles for the Detection of Ferritin Accumulation in Alzheimer's Disease. ACS Chemical Neuroscience, 2018, 9, 912-924.	3.5	49
57	Early neuromodulation prevents the development of brain and behavioral abnormalities in a rodent model of schizophrenia. Molecular Psychiatry, 2018, 23, 943-951.	7.9	36
58	Incorporation of Prior Knowledge of Signal Behavior Into the Reconstruction to Accelerate the Acquisition of Diffusion MRI Data. IEEE Transactions on Medical Imaging, 2018, 37, 547-556.	8.9	13
59	Suppression of 18F-FDG signal in the bladder on small animal PET-CT. PLoS ONE, 2018, 13, e0205610.	2.5	2
60	Surface scanning for 3D dose calculation in intraoperative electron radiation therapy. Radiation Oncology, 2018, 13, 243.	2.7	5
61	Stimulating the nucleus accumbens in obesity: A positron emission tomography study after deep brain stimulation in a rodent model. PLoS ONE, 2018, 13, e0204740.	2.5	11
62	MouBeAT: A New and Open Toolbox for Guided Analysis of Behavioral Tests in Mice. Frontiers in Behavioral Neuroscience, 2018, 12, 201.	2.0	28
63	Multicamera Optical Tracker Assessment for Computer Aided Surgery Applications. IEEE Access, 2018, 6, 64359-64370.	4.2	13
64	Enabling tomography with low-cost C-arm systems. PLoS ONE, 2018, 13, e0203817.	2.5	5
65	Understanding Deep Brain Stimulation: In Vivo Metabolic Consequences of the Electrode Insertional Effect. BioMed Research International, 2018, 2018, 1-6.	1.9	10
66	Unsupervised CT Lung Image Segmentation of a Mycobacterium Tuberculosis Infection Model. Scientific Reports, 2018, 8, 9802.	3.3	29
67	GPU-accelerated iterative reconstruction for limited-data tomography in CBCT systems. BMC Bioinformatics, 2018, 19, 171.	2.6	8
68	Deep brain stimulation electrode insertion and depression: Patterns of activity and modulation by analgesics. Brain Stimulation, 2018, 11, 1348-1355.	1.6	11
69	Total Variation Regularization With Split Bregman-Based Method in Magnetic Induction Tomography Using Experimental Data. IEEE Sensors Journal, 2017, 17, 976-985.	4.7	52
70	Optimized CUBIC protocol for 3D imaging of chicken embryos at single-cell resolution. Development (Cambridge), 2017, 144, 2092-2097.	2.5	35
71	Individual differences in the dominance of interhemispheric connections predict cognitive ability beyond sex and brain size. NeuroImage, 2017, 155, 234-244.	4.2	62
72	Insular pathology in young people with high-functioning autism and first-episode psychosis. Psychological Medicine, 2017, 47, 2472-2482.	4.5	29

#	Article	IF	CITATIONS
73	Subsurface Laser Engraving Techniques for Scintillator Crystals: Methods, Applications, and Advantages. IEEE Transactions on Radiation and Plasma Medical Sciences, 2017, 1, 377-384.	3.7	11
74	Pregnancy leads to long-lasting changes in human brain structure. Nature Neuroscience, 2017, 20, 287-296.	14.8	456
75	Medical Imaging Processing on a Big Data Platform Using Python: Experiences with Heterogeneous and Homogeneous Architectures. , 2017, , .		8
76	Differential Patterns of Subcortical Activity Evoked by Glial GLT-1 Blockade in Prelimbic and Infralimbic Cortex: Relationship to Antidepressant-Like Effects in Rats. International Journal of Neuropsychopharmacology, 2017, 20, 988-993.	2.1	17
77	Neurogenesis: Regulation by Alternative Splicing and Related Posttranscriptional Processes. Neuroscientist, 2017, 23, 466-477.	3.5	22
78	Assessment of intraoperative 3D imaging alternatives for IOERT dose estimation. Zeitschrift Fur Medizinische Physik, 2017, 27, 218-231.	1.5	19
79	ConoSurf: Openâ€source 3D scanning system based on a conoscopic holography device for acquiring surgical surfaces. International Journal of Medical Robotics and Computer Assisted Surgery, 2017, 13, e1788.	2.3	5
80	Looking inside the heart: a see-through view of the vascular tree. Biomedical Optics Express, 2017, 8, 3110.	2.9	21
81	FUX-Sim: Implementation of a fast universal simulation/reconstruction framework for X-ray systems. PLoS ONE, 2017, 12, e0180363.	2.5	13
82	Dronedarone produces early regression of myocardial remodelling in structural heart disease. PLoS ONE, 2017, 12, e0188442.	2.5	12
83	Technical Note: Mobile accelerator guidance using an optical tracker during docking in <scp>IOERT</scp> procedures. Medical Physics, 2017, 44, 5061-5069.	3.0	1
84	The miR-25-93-106b cluster regulates tumor metastasis and immune evasion via modulation of CXCL12 and PD-L1. Oncotarget, 2017, 8, 21609-21625.	1.8	72
85	Sparse reconstruction methods in x-ray CT. , 2017, , .		0
86	A Novel Prior- and Motion-Based Compressed Sensing Method for Small-Animal Respiratory Gated CT. PLoS ONE, 2016, 11, e0149841.	2.5	10
87	Response to Deep Brain Stimulation in Three Brain Targets with Implications in Mental Disorders: A PET Study in Rats. PLoS ONE, 2016, 11, e0168689.	2.5	8
88	3D imaging in CUBIC-cleared mouse heart tissue: going deeper. Biomedical Optics Express, 2016, 7, 3716.	2.9	33
89	Cortical morphometry in frontoparietal and default mode networks in mathâ€gifted adolescents. Human Brain Mapping, 2016, 37, 1893-1902.	3.6	16
90	The Disconnection Hypothesis inÂAlzheimer's Disease Studied Through Multimodal Magnetic Resonance Imaging: Structural, Perfusion, and Diffusion Tensor Imaging. Journal of Alzheimer's Disease, 2016, 50, 1051-1064.	2.6	15

#	Article	IF	CITATIONS
91	Deep brain stimulation improves behavior and modulates neural circuits in a rodent model of schizophrenia. Experimental Neurology, 2016, 283, 142-150.	4.1	48
92	Monitoring vascular normalization induced by antiangiogenic treatment with 18Fâ€fluoromisonidazoleâ€PET. Molecular Oncology, 2016, 10, 704-718.	4.6	36
93	3D imaging of the cleared intact murine colon with light sheet microscopy. , 2016, , .		Ο
94	Functional segmentation of dynamic PET studies: Open source implementation and validation of a leader-follower-based algorithm. Computers in Biology and Medicine, 2016, 69, 181-188.	7.0	1
95	Age at First Episode Modulates Diagnosis-Related Structural Brain Abnormalities in Psychosis. Schizophrenia Bulletin, 2016, 42, 344-357.	4.3	58
96	fMRat: an extension of SPM for a fully automatic analysis of rodent brain functional magnetic resonance series. Medical and Biological Engineering and Computing, 2016, 54, 743-752.	2.8	5
97	Automatic Cardiac Self-Gating of Small-Animal PET Data. Molecular Imaging and Biology, 2016, 18, 109-116.	2.6	5
98	Improved quantification for local regions of interest in preclinical PET imaging. Physics in Medicine and Biology, 2015, 60, 7127-7149.	3.0	9
99	Reproducibility of brain-cognition relationships using three cortical surface-based protocols: An exhaustive analysis based on cortical thickness. Human Brain Mapping, 2015, 36, 3227-3245.	3.6	31
100	Effects of chronic dietary exposure to monosodium glutamate on feeding behavior, adiposity, gastrointestinal motility, and cardiovascular function in healthy adult rats. Neurogastroenterology and Motility, 2015, 27, 1559-1570.	3.0	18
101	Stochastic effects in a discrete RT model with critical behaviour. Journal of Physics: Conference Series, 2015, 633, 012089.	0.4	0
102	Facial Onset Sensory and Motor Neuronopathy (FOSMN Syndrome) with abnormal brainstem neuroimaging: a case report. Journal of the Neurological Sciences, 2015, 357, e226-e227.	0.6	0
103	Fluorescence multi-scale endoscopy and its applications in the study and diagnosis of gastro-intestinal diseases: set-up design and software implementation. Proceedings of SPIE, 2015, , .	0.8	Ο
104	A labdane diterpene exerts ex vivo and in vivo cardioprotection against post-ischemic injury: Involvement of AKT-dependent mechanisms. Biochemical Pharmacology, 2015, 93, 428-439.	4.4	10
105	Detection of mouse endogenous type B astrocytes migrating towards brain lesions. Stem Cell Research, 2015, 14, 114-129.	0.7	13
106	The role of elastic restoring forces in right-ventricular filling. Cardiovascular Research, 2015, 107, 45-55.	3.8	15
107	Development and validation of an open source quantification tool for DSC-MRI studies. Computers in Biology and Medicine, 2015, 58, 56-62.	7.0	3
108	Gender effects on brain changes in early-onset psychosis. European Child and Adolescent Psychiatry, 2015, 24, 1193-1205.	4.7	7

#	Article	IF	CITATIONS
109	Intraoperative Electron-Beam Radiation Therapy for Pediatric Ewing Sarcomas and Rhabdomyosarcomas: Long-Term Outcomes. International Journal of Radiation Oncology Biology Physics, 2015, 92, 1069-1076.	0.8	12
110	Reduced Gyrification Is Related to Reduced Interhemispheric Connectivity in Autism Spectrum Disorders. Journal of the American Academy of Child and Adolescent Psychiatry, 2015, 54, 668-676.	0.5	37
111	Using a maternal immune stimulation model of schizophrenia to study behavioral and neurobiological alterations over the developmental course. Schizophrenia Research, 2015, 166, 238-247.	2.0	61
112	Exploitation of temporal redundancy in compressed sensing reconstruction of fMRI studies with a priorâ€based algorithm (PICCS). Medical Physics, 2015, 42, 3814-3821.	3.0	15
113	Functional neuroimaging of amphetamine-induced striatal neurotoxicity in the pleiotrophin knockout mouse model. Neuroscience Letters, 2015, 591, 132-137.	2.1	7
114	On feature extraction for noninvasive kernel estimation of left ventricular chamber function indices from echocardiographic images. , 2015, 39, 63-79.		0
115	Single-Institution Multidisciplinary Management of Locoregional Oligo-Recurrent Pelvic Malignancies: Long-Term Outcome Analysis. Annals of Surgical Oncology, 2015, 22, 1247-1255.	1.5	4
116	Sensationâ€ŧo ognition cortical streams in attentionâ€deficit/hyperactivity disorder. Human Brain Mapping, 2015, 36, 2544-2557.	3.6	44
117	Tissue-Dependent and Spatially-Variant Positron Range Correction in 3D PET. IEEE Transactions on Medical Imaging, 2015, 34, 2394-2403.	8.9	27
118	P.7.b.008 Progressive loss of gray matter volume in the frontal lobe is associated with decreased working memory performance over time in adolescent psychosis. European Neuropsychopharmacology, 2015, 25, S639-S640.	0.7	0
119	Predictors of schizophrenia spectrum disorders in early-onset first episodes of psychosis: a support vector machine model. European Child and Adolescent Psychiatry, 2015, 24, 427-440.	4.7	37
120	Investigation of Different Sparsity Transforms for the PICCS Algorithm in Small-Animal Respiratory Gated CT. PLoS ONE, 2015, 10, e0120140.	2.5	8
121	Abstract 1493: 18F-misonidazole PET (FMISO-PET) monitors vascular normalization (VN) and predicts benefit from antiangiogenic treatment plus chemotherapy in pancreas cancer. , 2015, , .		0
122	Comparison of Methods to Reduce Myocardial 18F-FDG Uptake in Mice: Calcium Channel Blockers versus High-Fat Diets. PLoS ONE, 2014, 9, e107999.	2.5	11
123	Added value of advanced over conventional magnetic resonance imaging in grading gliomas and other primary brain tumors. Cancer Imaging, 2014, 14, 35.	2.8	55
124	K-Ras ^{V14I} recapitulates Noonan syndrome in mice. Proceedings of the National Academy of Sciences of the United States of America, 2014, 111, 16395-16400.	7.1	67
125	White matter microstructure correlates of mathematical giftedness and intelligence quotient. Human Brain Mapping, 2014, 35, 2619-2631.	3.6	144
126	Application of the compressed sensing technique to selfâ€gated cardiac cine sequences in small animals. Magnetic Resonance in Medicine, 2014, 72, 369-380.	3.0	28

#	Article	IF	CITATIONS
127	Surfing the optimization space of a multiple-GPU parallel implementation of a X-ray tomography reconstruction algorithm. Journal of Systems and Software, 2014, 95, 166-175.	4.5	20
128	Cerebral Blood Flow is an Earlier Indicator of Perfusion Abnormalities than Cerebral Blood Volume in Alzheimer's Disease. Journal of Cerebral Blood Flow and Metabolism, 2014, 34, 654-659.	4.3	66
129	Dual-exposure technique for extending the dynamic range of x-ray flat panel detectors. Physics in Medicine and Biology, 2014, 59, 421-439.	3.0	9
130	Organ-focused mutual information for nonrigid multimodal registration of liver CT and Gd–EOB–DTPA-enhanced MRI. Medical Image Analysis, 2014, 18, 22-35.	11.6	13
131	In-line high resolution PET and 3T MRI hybrid device for preclinical multimodal imaging. EJNMMI Physics, 2014, 1, A7.	2.7	1
132	Cortical morphology of adolescents with bipolar disorder and with schizophrenia. Schizophrenia Research, 2014, 158, 91-99.	2.0	65
133	Response to Deep Brain Stimulation in the Lateral Hypothalamic Area in a Rat Model of Obesity: In Vivo Assessment of Brain Glucose Metabolism. Molecular Imaging and Biology, 2014, 16, 830-837.	2.6	30
134	Combination of Single-Photon Emission Computed Tomography and Magnetic Resonance Imaging to Track ¹¹¹ In-Oxine–Labeled Human Mesenchymal Stem Cells in Neuroblastoma-Bearing Mice. Molecular Imaging, 2014, 13, 7290.2014.00033.	1.4	15
135	Novel 4D image reconstruction for dynamic X-ray computed tomography in slow rotating scanners. , 2014, , .		0
136	Evaluation of the possibilities of limited angle reconstruction for the use of digital Radiography system as a tomograph. , 2014, , .		1
137	Compressed Sensing for Cardiac MRI Cine Sequences: A Real Implementation on a Small-Animal Scanner. IFMBE Proceedings, 2014, , 214-217.	0.3	1
138	A Prior-Based Image Variation (PRIVA) Approach Applied to Motion-Based Compressed Sensing Cardiac Cine MRI. IFMBE Proceedings, 2014, , 233-236.	0.3	2
139	Comparison of Total Variation with a Motion Estimation Based Compressed Sensing Approach for Self-Gated Cardiac Cine MRI in Small Animal Studies. PLoS ONE, 2014, 9, e110594.	2.5	16
140	Meningiomas: A Comparative Study of 68Ga-DOTATOC, 68Ga-DOTANOC and 68Ga-DOTATATE for Molecular Imaging in Mice. PLoS ONE, 2014, 9, e111624.	2.5	31
141	Optical Tracking System Integration into IORT Treatment Planning System. IFMBE Proceedings, 2014, , 37-40.	0.3	2
142	Parallel Implementation of a X-Ray Tomography Reconstruction Algorithm for High-Resolution Studies. IFMBE Proceedings, 2014, , 257-260.	0.3	0
143	Semi-automatic Segmentation of Sacrum in Computer Tomography Studies for Intraoperative Radiation Therapy. IFMBE Proceedings, 2014, , 344-347.	0.3	0
144	Massively parallelizable listâ€mode reconstruction using a Monte Carloâ€based elliptical Gaussian model. Medical Physics, 2013, 40, 012504.	3.0	6

#	Article	IF	CITATIONS
145	Positron range estimations with PeneloPET. Physics in Medicine and Biology, 2013, 58, 5127-5152.	3.0	56
146	Comparison of different methods of spatial normalization of FDG-PET brain images in the voxel-wise analysis of MCI patients and controls. Annals of Nuclear Medicine, 2013, 27, 600-609.	2.2	28
147	Behavioral, neurochemical and morphological changes induced by the overexpression of munc18-1a in brain of mice: relevance to schizophrenia. Translational Psychiatry, 2013, 3, e221-e221.	4.8	26
148	Automatic TAC extraction from dynamic cardiac PET imaging using iterative correlation from a population template. Computer Methods and Programs in Biomedicine, 2013, 111, 308-314.	4.7	3
149	MRI compatibility of position-sensitive photomultiplier depth-of-interaction PET detectors modules for in-line multimodality preclinical studies. Nuclear Instruments and Methods in Physics Research, Section A: Accelerators, Spectrometers, Detectors and Associated Equipment, 2013, 702, 83-87.	1.6	6
150	Use of Split Bregman denoising for iterative reconstruction in fluorescence diffuse optical tomography. Journal of Biomedical Optics, 2013, 18, 076016.	2.6	27
151	Feasibility of integrating a multi-camera optical tracking system in intra-operative electron radiation therapy scenarios. Physics in Medicine and Biology, 2013, 58, 8769-8782.	3.0	30
152	Improved dead-time correction for PET scanners: application to small-animal PET. Physics in Medicine and Biology, 2013, 58, 2059-2072.	3.0	7
153	Modification of the TASMIP x-ray spectral model for the simulation of microfocus x-ray sources. Medical Physics, 2013, 41, 011902.	3.0	9
154	The Human Cerebral Cortex Flattens during Adolescence. Journal of Neuroscience, 2013, 33, 15004-15010.	3.6	108
155	Parallel implementation of a X-ray tomography reconstruction algorithm based on MPI and CUDA. , 2013, , .		4
156	Diastolic chamber properties of the left ventricle assessed by global fitting of pressure-volume data: improving the gold standard of diastolic function. Journal of Applied Physiology, 2013, 115, 556-568.	2.5	19
157	Targeted Antifungal Prophylaxis in Heart Transplant Recipients. Transplantation, 2013, 96, 664-669.	1.0	46
158	jClustering, an Open Framework for the Development of 4D Clustering Algorithms. PLoS ONE, 2013, 8, e70797.	2.5	3
159	Is the Cerebellum the Optimal Reference Region for Intensity Normalization of Perfusion MR Studies in Early Alzheimer's Disease?. PLoS ONE, 2013, 8, e81548.	2.5	14
160	Progressive Brain Changes in Children and Adolescents With First-Episode Psychosis. Archives of General Psychiatry, 2012, 69, 16.	12.3	135
161	Misalignments calibration in small-animal PET scanners based on rotating planar detectors and parallel-beam geometry. Physics in Medicine and Biology, 2012, 57, 7493-7518.	3.0	4
162	A method for small-animal PET/CT alignment calibration. Physics in Medicine and Biology, 2012, 57, N199-N207.	3.0	9

#	Article	IF	CITATIONS
163	Investigation of different Compressed Sensing approaches for respiratory gating in small animal CT. , 2012, , .		3
164	Influence of absorption and scattering on the quantification of fluorescence diffuse optical tomography using normalized data. Journal of Biomedical Optics, 2012, 17, 036013.	2.6	14
165	Regional specificity of thalamic volume deficits in male adolescents with early-onset psychosis. British Journal of Psychiatry, 2012, 200, 30-36.	2.8	23
166	Approach to Assessing Myocardial Perfusion in Rats Using Static [13N]-Ammonia Images and a Small-Animal PET. Molecular Imaging and Biology, 2012, 14, 541-545.	2.6	5
167	An Innovative Tool for Intraoperative Electron Beam Radiotherapy Simulation and Planning: Description and Initial Evaluation by Radiation Oncologists. International Journal of Radiation Oncology Biology Physics, 2012, 83, e287-e295.	0.8	56
168	Exploiting Parallelism in a X-ray Tomography Reconstruction Algorithm on Hybrid Multi-GPU and Multi-core Platforms. , 2012, , .		4
169	Accuracy of CT-based attenuation correction in PET/CT bone imaging. Physics in Medicine and Biology, 2012, 57, 2477-2490.	3.0	40
170	Two weeks of postsurgical therapy may be enough for high-risk cases of endocarditis caused by Streptococcus viridans or Streptococcus bovis. Clinical Microbiology and Infection, 2012, 18, 293-299.	6.0	15
171	Software architecture for multi-bed FDK-based reconstruction in X-ray CT scanners. Computer Methods and Programs in Biomedicine, 2012, 107, 218-232.	4.7	37
172	Poster #40 LONGITUDINAL CHANGE IN LEVELS OF N-ACETYL-ASPARTATE IN EARLY ONSET PSYCHOSIS AND HEALTHY CONTROLS. Schizophrenia Research, 2012, 136, S106.	2.0	0
173	Decreased glutathione levels predict loss of brain volume in children and adolescents with first-episode psychosis in a two-year longitudinal study. Schizophrenia Research, 2012, 137, 58-65.	2.0	50
174	Live Imaging of Mouse Endogenous Neural Progenitors Migrating in Response to an Induced Tumor. PLoS ONE, 2012, 7, e44466.	2.5	20
175	Waking-like Brain Function in Embryos. Current Biology, 2012, 22, 852-861.	3.9	30
176	Comparative evaluation of autofocus algorithms for a realâ€ŧime system for automatic detection of <i>Mycobacterium tuberculosis</i> . Cytometry Part A: the Journal of the International Society for Analytical Cytology, 2012, 81A, 213-221.	1.5	41
177	Quantification limits of iterative PET reconstruction algorithms and improved estimation of kinetic constants. , 2011, , .		1
178	GPU-Based Fast Iterative Reconstruction of Fully 3-D PET Sinograms. IEEE Transactions on Nuclear Science, 2011, 58, 2257-2263.	2.0	29
179	Leader-follower clustering algorithm for automatic segmentation of cardiac PET studies. , 2011, , .		3
180	Mathematically gifted adolescents use more extensive and more bilateral areas of the fronto-parietal network than controls during executive functioning and fluid reasoning tasks. NeuroImage, 2011, 57, 281-292.	4.2	65

#	Article	IF	CITATIONS
181	28 poster INTRAOPERATIVE ELECTRON RADIATION THERAPY PREPLANNING USING RADIANCE NEW FEATURES. THE NEED FOR COMMON PROTOCOLS REVISITED. Radiotherapy and Oncology, 2011, 99, S14.	0.6	0
182	Split operator method for fluorescence diffuse optical tomography using anisotropic diffusion regularisation with prior anatomical information. Biomedical Optics Express, 2011, 2, 2632.	2.9	38
183	Feasibility of U-curve method to select the regularization parameter for fluorescence diffuse optical tomography in phantom and small animal studies. Optics Express, 2011, 19, 11490.	3.4	32
184	Liver Segmentation and Volume Estimation from Preoperative CT Images in Hepatic Surgical Planning: Application of a Semiautomatic Method Based on 3D Level Sets. , 2011, , .		2
185	Fluorescence diffuse optical tomography using the split Bregman method. Medical Physics, 2011, 38, 6275-6284.	3.0	57
186	Study of CT-based positron range correction in high resolution 3D PET imaging. Nuclear Instruments and Methods in Physics Research, Section A: Accelerators, Spectrometers, Detectors and Associated Equipment, 2011, 648, S172-S175.	1.6	18
187	Fully 3D GPU PET reconstruction. Nuclear Instruments and Methods in Physics Research, Section A: Accelerators, Spectrometers, Detectors and Associated Equipment, 2011, 648, S169-S171.	1.6	8
188	A novel approach to investigate neuronal network activity patterns affected by deep brain stimulation in rats. Journal of Psychiatric Research, 2011, 45, 927-930.	3.1	23
189	Influence of resting energy expenditure on weight gain in adolescents taking second-generation antipsychotics. Clinical Nutrition, 2011, 30, 616-623.	5.0	32
190	Chronic Cannabinoid Administration to Periadolescent Rats Modulates the Metabolic Response to Acute Cocaine in the Adult Brain. Molecular Imaging and Biology, 2011, 13, 411-415.	2.6	11
191	The application of nanoparticles in gene therapy and magnetic resonance imaging. Microscopy Research and Technique, 2011, 74, 577-591.	2.2	40
192	Variations in the shape of the frontobasal brain region in obsessive-compulsive disorder. Human Brain Mapping, 2011, 32, 1100-1108.	3.6	14
193	NEMA NU 4-2008 Performance Measurements of Two Commercial Small-Animal PET Scanners: ClearPET and rPET-1. IEEE Transactions on Nuclear Science, 2011, 58, 58-65.	2.0	31
194	Optimal multiresolution 3D level-set method for liver segmentation incorporating local curvature constraints. , 2011, 2011, 3419-22.		14
195	Multicenter Study of Brain Volume Abnormalities in Children and Adolescent-Onset Psychosis. Schizophrenia Bulletin, 2011, 37, 1270-1280.	4.3	28
196	Constitutive activation of B-Raf in the mouse germ line provides a model for human cardio-facio-cutaneous syndrome. Proceedings of the National Academy of Sciences of the United States of America, 2011, 108, 5015-5020.	7.1	61
197	Performance Evaluation of SiPM Photosensors in the Presence of Magnetic Fields. AIP Conference Proceedings, 2010, , .	0.4	0
198	Performance evaluation of SiPM photodetectors for PET imaging in the presence of magnetic fields. Nuclear Instruments and Methods in Physics Research, Section A: Accelerators, Spectrometers, Detectors and Associated Equipment, 2010, 613, 308-316.	1.6	56

#	Article	IF	CITATIONS
199	Dopamine D4 receptors modulate brain metabolic activity in the prefrontal cortex and cerebellum at rest and in response to methylphenidate. European Journal of Neuroscience, 2010, 32, 668-676.	2.6	26
200	New Murine Sub-massive Pulmonary Embolism Model, Sensitive To Both Clinical Treatments And Diagnostic Techniques. , 2010, , .		0
201	Performance evaluation for ⁶⁸ Ga and ¹⁸ F of the ARGUS small-animal PET scanner based on the NEMA NU-4 standard. , 2010, , .		6
202	Iterative automatic segmentation in cardiac PET based on TAC correlation: Preliminary results. , 2010, ,		0
203	Validation of PeneloPET positron range estimations. , 2010, , .		4
204	Data acquisition electronics for gamma ray emission tomography using width-modulated leading-edge discriminators. Physics in Medicine and Biology, 2010, 55, 4291-4308.	3.0	3
205	FRONTAL CORTICAL THICKNESS IS ASSOCIATED WITH CLINICAL IMPROVEMENT OF NEGATIVE SYMPTOMS IN MALE ADOLESCENTS WITH EARLY-ONSET FIRST-EPISODE PSYCHOSIS. Schizophrenia Research, 2010, 117, 225-226.	2.0	1
206	FRONTAL CORTICAL THICKNESS IS ASSOCIATED WITH CLINICAL IMPROVEMENT OF NEGATIVE SYMPTOMS IN MALE ADOLESCENTS WITH EARLY-ONSET FIRST-EPISODE PSYCHOSIS. Schizophrenia Research, 2010, 117, 227-228.	2.0	0
207	A SPECT Scanner for Rodent Imaging Based on Small-Area Gamma Cameras. IEEE Transactions on Nuclear Science, 2010, 57, 2524-2531.	2.0	4
208	Effects of the Super Bialkali Photocathode on the Performance Characteristics of a Position-Sensitive Depth-of-Interaction PET Detector Module. IEEE Transactions on Nuclear Science, 2010, 57, 2437-2441.	2.0	5
209	Validation of NEMA NU4–2008 scatter fraction estimation with ¹⁸ F and ⁶⁸ Ga for the ARGUS smallanimal PET scanner. , 2010, , .		1
210	GPU acceleration of a fully 3D Iterative Reconstruction Software for PET using CUDA. , 2009, , .		8
211	3D liver segmentation in preoperative CT images using a levelsets active surface method. , 2009, 2009, 3625-8.		16
212	FDOT reconstruction and setting optimization using singular value analysis with automatic thresholding. , 2009, , .		1
213	Positron range effects in high resolution 3D PET imaging. , 2009, , .		17
214	rSPECT: A compact gamma camera based SPECT system for small-animal imaging. , 2009, , .		0
215	Automated dual-exposure technique to extend the dynamic range of flat-panel detectors used in small-animal cone-beam micro-CT. , 2009, , .		0
216	Brain morphology and neurological soft signs in adolescents with first-episode psychosis. British Journal of Psychiatry, 2009, 195, 227-233.	2.8	50

#	Article	IF	CITATIONS
217	Design and performance evaluation of a coplanar multimodality scanner for rodent imaging. Physics in Medicine and Biology, 2009, 54, 5427-5441.	3.0	49
218	Progression of Brain Volume Changes in Adolescent-Onset Psychosis. Schizophrenia Bulletin, 2009, 35, 233-243.	4.3	48
219	A novel R-package graphic user interface for the analysis of metabonomic profiles. BMC Bioinformatics, 2009, 10, 363.	2.6	54
220	Assessment of the increase in variability when combining volumetric data from different scanners. Human Brain Mapping, 2009, 30, 355-368.	3.6	48
221	Automatic quantification of histological studies in allergic asthma. Cytometry Part A: the Journal of the International Society for Analytical Cytology, 2009, 75A, 271-277.	1.5	2
222	Automated Method for Small-Animal PET Image Registration with Intrinsic Validation. Molecular Imaging and Biology, 2009, 11, 107-113.	2.6	29
223	Detection of Visual Activation in the Rat Brain Using 2-deoxy-2-[18F]fluoro-d-glucose and Statistical Parametric Mapping (SPM). Molecular Imaging and Biology, 2009, 11, 94-99.	2.6	22
224	Assessment of Airway Distribution of Transnasal Solutions in Mice by PET/CT Imaging. Molecular Imaging and Biology, 2009, 11, 263-268.	2.6	6
225	Incidence and risk factors for ventilator-associated pneumonia after major heart surgery. Intensive Care Medicine, 2009, 35, 1518-1525.	8.2	129
226	Gyral and Sulcal Cortical Thinning in Adolescents with First Episode Early-Onset Psychosis. Biological Psychiatry, 2009, 66, 1047-1054.	1.3	45
227	Sinogram bowâ€tie filtering in FBP PET reconstruction. Medical Physics, 2009, 36, 1663-1671.	3.0	11
228	fMRI study of math-gifted adolescents and controls while performing the Raven Progressive Matrices task. NeuroImage, 2009, 47, S111.	4.2	0
229	PeneloPET, a Monte Carlo PET simulation tool based on PENELOPE: features and validation. Physics in Medicine and Biology, 2009, 54, 1723-1742.	3.0	76
230	The Chemokine Receptor CXCR4 and the Metalloproteinase MT1-MMP Are Mutually Required during Melanoma Metastasis to Lungs. American Journal of Pathology, 2009, 174, 602-612.	3.8	74
231	Multipurpose Monte Carlo simulator for photon transport in turbid media. , 2009, , .		0
232	Mapping the Thalamus in Adolescents with First Episode Psychosis. NeuroImage, 2009, 47, S135.	4.2	0
233	Unsupervised estimation of myocardial displacement from tagged MR sequences using nonrigid registration. Magnetic Resonance in Medicine, 2008, 59, 181-189.	3.0	34
234	A New Method for the Rapid Synthesis of Water Stable Superparamagnetic Nanoparticles. Chemistry - A European Journal, 2008, 14, 9126-9130.	3.3	32

#	Article	IF	CITATIONS
235	Gray matter deficits in bipolar disorder are associated with genetic variability at interleukinâ€1 beta gene (2q13). Genes, Brain and Behavior, 2008, 7, 796-801.	2.2	54
236	Differences in response to food stimuli in a rat model of obesity: in-vivo assessment of brain glucose metabolism. International Journal of Obesity, 2008, 32, 1171-1179.	3.4	42
237	Differential clinical, structural and P300 parameters in schizophrenia patients resistant to conventional neuroleptics. Progress in Neuro-Psychopharmacology and Biological Psychiatry, 2008, 32, 257-266.	4.8	29
238	Regional Gray Matter Volume Deficits in Adolescents With First-Episode Psychosis. Journal of the American Academy of Child and Adolescent Psychiatry, 2008, 47, 1311-1320.	0.5	77
239	Assessment of a New High-Performance Small-Animal X-Ray Tomograph. IEEE Transactions on Nuclear Science, 2008, 55, 898-905.	2.0	48
240	Performance comparison of two commercial small animal PET scanners: ClearPETT and rPET-1T. , 2008, , .		3
241	Validation of a retrospective respiratory gating method for small-animal CT scanners. , 2008, , .		3
242	Augmented Acquisition of Cocaine Self-Administration and Altered Brain Glucose Metabolism in Adult Female but not Male Rats Exposed to a Cannabinoid Agonist during Adolescence. Neuropsychopharmacology, 2008, 33, 806-813.	5.4	82
243	Extraction of the respiratory signal from small-animal CT projections for a retrospective gating method. Physics in Medicine and Biology, 2008, 53, 4683-4695.	3.0	11
244	Frequency selective signal extrapolation for compensation of missing data in sinograms. , 2008, , .		8
245	Efficient methodology for 3D statistical reconstruction of high resolution coplanar PET/CT scanner. , 2008, , .		1
246	PET/CT alignment for small animal scanners based on capillary detection. , 2008, , .		2
247	Fully 4D reconstruction of dynamic SPECT images based on the estimation of spatiotemporal basis coefficients directly from projection measurements. , 2008, , .		0
248	VrPET/CT: Development of a rotating multimodality scanner for small-animal imaging. , 2008, , .		4
249	Nonlinear effect of pile-up in the quantification of a small animal PET scanner. , 2008, , .		Ο
250	Performance evaluation of SiPM detectors for PET imaging in the presence of magnetic fields. , 2008, , .		13
251	Use of IBASPM atlas-based automatic segmentation toolbox in pathological brains: Effect of template selection. , 2008, , .		2
252	Comparative study of two flat-panel X-ray detectors applied to small-animal imaging cone-beam		2

micro-CT., 2008, , .

#	Article	IF	CITATIONS
253	Effects of the Super Bialkali photocathode on the performance characteristics of a position-sensitive depth-of-interaction PET detector module. , 2008, , .		2
254	Design and development of a co-planar fluorescence and X-ray tomograph. , 2008, , .		2
255	Real-Time Digital Timing in Positron Emission Tomography. IEEE Transactions on Nuclear Science, 2008, 55, 2531-2540.	2.0	21
256	A super-resolution feasibility study in small-animal SPECT imaging. , 2008, , .		4
257	Longitudinal Brain Changes in Early-Onset Psychosis. Schizophrenia Bulletin, 2007, 34, 341-353.	4.3	76
258	1H MR Spectroscopy in the Assessment of Gliomatosis Cerebri. American Journal of Roentgenology, 2007, 188, 710-714.	2.2	38
259	Changes in Cortical Volume with Olanzapine in Chronic Schizophrenia. Pharmacopsychiatry, 2007, 40, 135-139.	3.3	15
260	Validation of PeneloPET against two small animal PET scanners. , 2007, , .		4
261	PETonCHIP: architecture of a on-chip high-resolution, fully digital positron emission tomography scanner for small Animal Imaging. , 2007, , .		3
262	Small-animal PET registration method with intrinsic validation designed for large datasets. , 2007, , .		1
263	Dorsolateral prefrontal <i>N</i> -acetyl-aspartate concentration in male patients with chronic schizophrenia and with chronic bipolar disorder. European Psychiatry, 2007, 22, 505-512.	0.2	56
264	Impact of ventricular enlargement on the measurement of metabolic activity in spatially normalized PET. NeuroImage, 2007, 35, 748-758.	4.2	17
265	The child and adolescent first-episode psychosis study (CAFEPS): Design and baseline results. Schizophrenia Research, 2007, 91, 226-237.	2.0	85
266	Radial Versus Longitudinal Myocardial Deformation from Gray-Scale Echocardiography. Ultrasound in Medicine and Biology, 2007, 33, 1699-1705.	1.5	0
267	Linezolid therapy for infective endocarditis. Clinical Microbiology and Infection, 2007, 13, 211-215.	6.0	54
268	Findings of proton magnetic resonance spectometry in the dorsolateral prefrontal cortex in adolescents with first episodes of psychosis. Psychiatry Research - Neuroimaging, 2007, 156, 33-42.	1.8	27
269	Effects of MDMA on blood glucose levels and brain glucose metabolism. European Journal of Nuclear Medicine and Molecular Imaging, 2007, 34, 916-925.	6.4	20
270	Noise and physical limits to maximum resolution of PET images. Nuclear Instruments and Methods in Physics Research, Section A: Accelerators, Spectrometers, Detectors and Associated Equipment, 2007, 580, 934-937.	1.6	4

#	Article	IF	CITATIONS
271	New embedded digital front-end for high resolution PET scanner. IEEE Transactions on Nuclear Science, 2006, 53, 770-775.	2.0	18
272	Design an development of a high performance micro-CT system for small animal imaging. , 2006, , .		3
273	Optimal and Robust PET Data Sinogram Restoration Based on the Response of the System. , 2006, , .		2
274	The novel DNA methylation inhibitor zebularine is effective against the development of murine T-cell lymphoma. Blood, 2006, 107, 1174-1177.	1.4	64
275	Automatic identification of Mycobacterium tuberculosis by Gaussian mixture models. Journal of Microscopy, 2006, 223, 120-132.	1.8	70
276	Cardiac motion analysis from ultrasound sequences using nonrigid registration: Validation against Doppler tissue velocity. Ultrasound in Medicine and Biology, 2006, 32, 483-490.	1.5	50
277	Minimum-norm reconstruction for sensitivity-encoded magnetic resonance spectroscopic imaging. Magnetic Resonance in Medicine, 2006, 55, 287-295.	3.0	38
278	Normalization in 3D PET: Dependence on the Activity Distribution of the Source. , 2006, , .		1
279	Digital timing in positron emission tomography. , 2006, , .		2
280	FIRST: Fast Iterative Reconstruction Software for (PET) tomography. Physics in Medicine and Biology, 2006, 51, 4547-4565.	3.0	86
281	Usefulness of quantitative myocardial contrast echocardiography for prediction of ventricular function recovery after myocardial infarction treated with primary angioplasty. Heart, 2006, 92, 693-694.	2.9	3
282	Modeling the acquisition front-end in high resolution gamma-ray imaging. IEEE Transactions on Nuclear Science, 2006, 53, 1150-1155.	2.0	9
283	Hypofrontality in men with first-episode psychosis. British Journal of Psychiatry, 2005, 186, 203-208.	2.8	34
284	B27 ADOLESCENT CANNABINOID PRE-EXPOSURE EFFECTS ON COCAINE SELF-ADMINISTRATION, FOOD REINFORCED BEHAVIOR AND CEREBRAL GLUCOSE METABOLISM IN ADULT RATS. Behavioural Pharmacology, 2005, 16, S74.	1.7	0
285	Olanzapine-induced cerebral metabolic changes related to symptom improvement in schizophrenia. International Clinical Psychopharmacology, 2005, 20, 13-18.	1.7	21
286	The expression of GLP-1 receptor mRNA and protein allows the effect of GLP-1 on glucose metabolism in the human hypothalamus and brainstem. Journal of Neurochemistry, 2005, 92, 798-806.	3.9	241
287	Cerebral metabolic changes induced by clozapine in schizophrenia and related to clinical improvement. Psychopharmacology, 2005, 178, 17-26.	3.1	65
288	Age-related intramyocardial patterns in healthy subjects evaluated with Doppler tissue imaging. European Journal of Echocardiography, 2005, 6, 175-185.	2.3	10

#	Article	IF	CITATIONS
289	ROC evaluation of statistical wavelet-based analysis of brain activation in [150]-H2O PET scans. NeuroImage, 2005, 24, 763-770.	4.2	5
290	Ventricular enlargement in schizophrenia is associated with a genetic polymorphism at the interleukin-1 receptor antagonist gene. NeuroImage, 2005, 27, 1002-1006.	4.2	46
291	Structural Neuroimaging in Adolescents With a First Psychotic Episode. Journal of the American Academy of Child and Adolescent Psychiatry, 2005, 44, 1151-1157.	0.5	37
292	Spatio-temporal nonrigid registration for ultrasound cardiac motion estimation. IEEE Transactions on Medical Imaging, 2005, 24, 1113-1126.	8.9	243
293	N-acetyl-aspartate levels in the dorsolateral prefrontal cortex in the early years of schizophrenia are inversely related to disease duration. Schizophrenia Research, 2005, 73, 209-219.	2.0	58
294	Increase in gray matter and decrease in white matter volumes in the cortex during treatment with atypical neuroleptics in schizophrenia. Schizophrenia Research, 2005, 80, 61-71.	2.0	99
295	MÃ;s de un siglo de imagen médica. Arbor, 2004, CLXXVII, 337-364.	0.3	1
296	Quantification Methods in Contrast Echocardiography. , 2004, , 69-89.		0
297	A European perspective on intravascular catheter-related infections: report on the microbiology workload, aetiology and antimicrobial susceptibility (ESCNI-005 Study). Clinical Microbiology and Infection, 2004, 10, 838-842.	6.0	44
298	Clinical-epidemiological characteristics and outcome of patients with catheter-related bloodstream infections in Europe (ESGNI-006 Study). Clinical Microbiology and Infection, 2004, 10, 843-845.	6.0	19
299	Risk Factors of Invasive Aspergillosis after Heart Transplantation: Protective Role of Oral Itraconazole Prophylaxis. American Journal of Transplantation, 2004, 4, 636-643.	4.7	110
300	18F-FDG positron emission tomography staging and restaging in rectal cancer treated with preoperative chemoradiation. International Journal of Radiation Oncology Biology Physics, 2004, 58, 528-535.	0.8	168
301	Resolution recovery in Turbo Spin Echo using segmented Half Fourier acquisition. Magnetic Resonance Imaging, 2004, 22, 369-378.	1.8	2
302	Method for bias field correction of brain T1-weighted magnetic resonance images minimizing segmentation error. Human Brain Mapping, 2004, 22, 133-144.	3.6	65
303	Tracking of regions-of-interest in myocardial contrast echocardiography. Ultrasound in Medicine and Biology, 2004, 30, 303-309.	1.5	31
304	Usefulness of Tc-99m RBC SPECT/MRI Fusion Imaging in Small Suspected Hepatic Hemangiomas. Clinical Nuclear Medicine, 2004, 29, 844-845.	1.3	4
305	Cerebral metabolic patterns in chronic and recent-onset schizophrenia. Psychiatry Research - Neuroimaging, 2003, 122, 125-135.	1.8	53
306	Anatomical and functional cerebral variables associated with basal symptoms but not risperidone response in minimally treated schizophrenia. Psychiatry Research - Neuroimaging, 2003, 124, 163-175.	1.8	34

#	Article	IF	CITATIONS
307	Anatomical and functional brain variables associated with clozapine response in treatment-resistant schizophrenia. Psychiatry Research - Neuroimaging, 2003, 124, 153-161.	1.8	70
308	Automatic quantification of viability in epithelial cell cultures by texture analysis. Journal of Microscopy, 2003, 209, 34-40.	1.8	13
309	New Techniques for the Assessment of Regional Left Ventricular Wall Motion. Echocardiography, 2003, 20, 659-672.	0.9	16
310	Cerebral metabolism and risperidone treatment in schizophrenia. Schizophrenia Research, 2003, 60, 1-7.	2.0	41
311	Influence of the normalization template on the outcome of statistical parametric mapping of PET scans. NeuroImage, 2003, 19, 601-612.	4.2	125
312	Mapas de estadÃsticos paramétricos (SPM) en medicina nuclear. Revista Española De Medicina Nuclear, 2003, 22, 43-53.	0.3	2
313	Segmentation, autofocusing and signagture extraction of tuberculosis sputum images. , 2002, 4788, 171.		14
314	Association between relative temporal and prefrontal sulcal cerebrospinal fluid and illness duration in schizophrenia. Schizophrenia Research, 2002, 58, 305-312.	2.0	21
315	Intramyocardial analysis of regional systolic and diastolic function in ischemic heart disease with Doppler tissue imaging: Role of the different myocardial layers. Journal of the American Society of Echocardiography, 2002, 15, 99-108.	2.8	25
316	Biological dosimetry of magnetic resonance imaging. Journal of Magnetic Resonance Imaging, 2002, 15, 584-590.	3.4	13
317	Assessment of normal and ischaemic myocardium by quantitative m-mode tissue doppler imaging. Ultrasound in Medicine and Biology, 2002, 28, 561-569.	1.5	18
318	Multimodal neuroimaging studies and neurodevelopment and neurodegeneration hypotheses of schizophrenia. Neurotoxicity Research, 2002, 4, 437-451.	2.7	5
319	P300 amplitude as a possible correlate of frontal degeneration in schizophrenia. Schizophrenia Research, 2001, 49, 121-128.	2.0	40
320	<title>Automatic sputum color image segmentation for tuberculosis diagnosis</title> ., 2001, , .		15
321	PET, CT, and MR image registration of the rat brain and skull. IEEE Transactions on Nuclear Science, 2001, 48, 1440-1445.	2.0	36
322	<title>Multimodality image quantification using the Talairach grid</title> . , 2001, , .		28
323	<title>Neurosurgery for functional disorders guided by multimodality imaging</title> . , 2001, , .		0
324	<title>Myocardial perfusion assessment with contrast echocardiography</title> .,2001,,.		4

#	Article	IF	CITATIONS
325	<title>Multimodality image integration for radiotherapy treatment: an easy approach</title> . , 2001, , .		Ο
326	<title>Automatic detection of cellular necrosis in epithelial cell cultures</title> .,2001,,.		9
327	<title>Multimodality localization of epileptic foci</title> ., 2001, 4321, 362.		5
328	Multiresolution analysis in fMRI: Sensitivity and specificity in the detection of brain activation. Human Brain Mapping, 2001, 14, 16-27.	3.6	43
329	<title>Accuracy of heart strain rate calculation derived from Doppler tissue velocity data</title> . , 2001, 4325, 546.		3
330	<title>Statistical segmentation of multidimensional brain datasets</title> ., 2001, , .		11
331	Paradoxical Effects of Temperature on Vascular Tone. Cryobiology, 2000, 41, 43-50.	0.7	17
332	19. Correlation between FDG PET data and EEG dipole modeling. Molecular Imaging and Biology, 2000, 3, 173.	0.3	6
333	Regional diastolic function in ischaemic heart disease using pulsed wave Doppler tissue imaging. European Heart Journal, 1999, 20, 496-505.	2.2	168
334	Simulated Surgery on Computed Tomography and Magnetic Resonance Images: An Aid for Intraoperative Radiotherapy. Computer Aided Surgery, 1997, 2, 333-339.	1.8	3
335	Postsurgical Mediastinitis: A Case ontrol Study. Clinical Infectious Diseases, 1997, 25, 1060-1064.	5.8	120
336	Simulated surgery on computed tomography and magnetic resonance images: An aid for intraoperative radiotherapy. Computer Aided Surgery, 1997, 2, 333-339.	1.8	3
337	Development and Clinical Assay of the BCM Ventricular Assist Device. Artificial Organs, 1994, 18, 484-489.	1.9	6
338	Immunological and serological markers predictive of progression to AIDS in a cohort of HIV-infected drug users. Aids, 1990, 4, 987-994.	2.2	63
339	Quality assurance in radiation therapy: Systematic evaluation of errors during the treatment execution. Radiotherapy and Oncology, 1987, 8, 253-261.	0.6	22
340	Co-Planar PET/CT for Small Animal Imaging. , 0, , .		5
341	Statistical Reconstruction Methods in PET: Resolution Limit, Noise, Edge Artifacts and considerations for the design of better scanners. , 0, , .		5
342	Quasi Pseudo-Inverse Reconstruction Technique for Rotating PET Scanners. , 0, , .		1

#	Article	IF	CITATIONS
343	rPET Detectors Design and Data Processing. , 0, , .		24